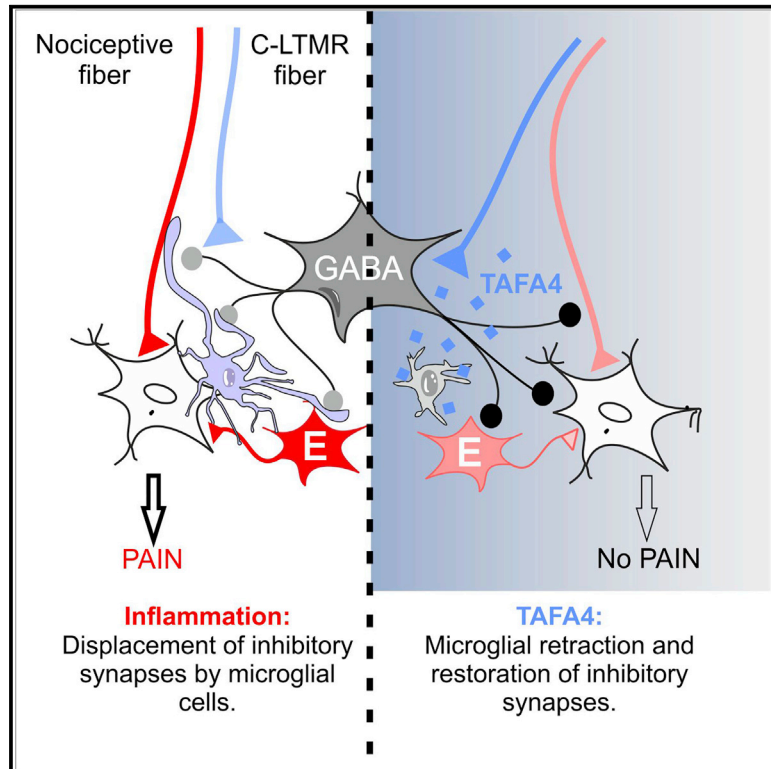


## TFAFA4 Reverses Mechanical Allodynia through Activation of GABAergic Transmission and Microglial Process Retraction

### Graphical Abstract



### Authors

Charline Kambrun, Olivier Roca-Lapirot, Chiara Salio, Marc Landry, Aziz Moqrich, Yves Le Feuvre

### Correspondence

yves.le-feuvre@u-bordeaux.fr

### In Brief

TFAFA4 is a recently discovered chemokine secreted by C-low-threshold mechanoreceptors (C-LTMRs). Kambrun et al. describe the interplay between C-LTMRs, spinal GABAergic neurons, and microglial cells that is responsible for the mechanical pain alleviation induced by TFAFA4 by inflammation.

### Highlights

- C-LTMR neurons contact GABAergic neurons
- TFAFA4, a chemokine secreted by C-LMTR, promotes microglial process retraction
- TFAFA4 enables restoration of inhibitory inputs to spinal neurons
- TFAFA4 attenuates nociceptive transmission in the spinal cord



# TFAA4 Reverses Mechanical Allodynia through Activation of GABAergic Transmission and Microglial Process Retraction

Charline Kambrun,<sup>1,2</sup> Olivier Roca-Lapirot,<sup>1,2</sup> Chiara Salio,<sup>3</sup> Marc Landry,<sup>1,2</sup> Aziz Moqrich,<sup>4</sup> and Yves Le Feuvre<sup>1,2,5,\*</sup>

<sup>1</sup>Interdisciplinary Institute for Neuroscience, University Bordeaux, UMR 5297, 33000 Bordeaux, France

<sup>2</sup>Interdisciplinary Institute for Neuroscience, CNRS, UMR 5297, 33000 Bordeaux, France

<sup>3</sup>Department of Veterinary Sciences, University of Turin, 10095 Grugliasco (TO), Italy

<sup>4</sup>Aix-Marseille-Université, CNRS, Institut de Biologie du Développement de Marseille, UMR 7288, Case 907, 13288 Cedex 09, France

<sup>5</sup>Lead Contact

\*Correspondence: [yves.le-feuvre@u-bordeaux.fr](mailto:yves.le-feuvre@u-bordeaux.fr)

<https://doi.org/10.1016/j.celrep.2018.02.068>

## SUMMARY

C-low-threshold mechanoreceptors (C-LTMRs) are sensory neurons that, beyond conveying pleasant touch, modulate nociceptive transmission within the spinal cord. However, pain alleviation by C-LTMRs remains poorly understood. Here, we show that the C-LTMR-derived TFAA4 chemokine induces a reinforcement of inhibitory synaptic transmission within spinal networks, which consequently depresses local excitatory synapses and impairs synaptic transmission from high-threshold C-fibers. In animals with inflammation induced by Freund's complete adjuvant, TFAA4 decreases the noxious stimulus-induced neuronal responses recorded *in vivo* and alleviates mechanical pain. Both effects are blocked by antagonists of GABAergic transmission. Furthermore, TFAA4 promotes microglial retraction in inflammation and increases the number of inhibitory synapses on lamina III somata. Altogether, these results demonstrate GABAergic interneurons to be the first integration relay for C-LTMRs and highlight a tight interplay between sensory neurons, microglial cells, and spinal interneurons, which fine-tunes inhibitory activity and nociceptive transmission in pathological conditions.

## INTRODUCTION

Acute pain is an alarm signal allowing behavioral adaptation in response to potentially harmful stimuli. However, in pathological conditions, acute pain can turn into chronic maladaptive pain, which results from central sensitization of dorsal spinal networks (Latremoliere and Woolf, 2009; Woolf, 2011). A large body of work has shown the key role played by the disinhibition of dorsal spinal networks in chronic pain pathologies (Guo and Hu, 2014; Lin et al., 1996; Taylor, 2009). Specifically, nerve injury or inflammation can lead to a loss of GABAergic inhibition (Moore et al., 2002; Laffray et al., 2012; Zhang et al., 2013). For instance, mi-

croglial cells are known to regulate the strength of inhibitory synapses through an attenuation of chloride gradients (Coull et al., 2005). Microglia also modulate inhibitory transmission by the release of proinflammatory cytokines (Kawasaki et al., 2008). Thus, many forms of pathological pain may result from an impairment of the fragile interplay between inhibitory synapses and the surrounding glial cells, making its alleviation very challenging.

Since the pioneering work of Melzack and Wall (1965), inhibitory networks in the spinal cord have been thought to be tightly driven by low-threshold peripheral inputs (Daniele and MacDermott, 2009; Takazawa and MacDermott, 2010). In pathological pain, this drive is thought to be deficient (Leitner et al., 2013; Lu et al., 2013; Sdrulla et al., 2015), thus leading to a weakening of inhibitory activity, which may, in turn, reinforce nociceptive transmission. Among the low-threshold inputs, recent attention has been paid to C-low-threshold mechanoreceptors (C-LTMRs) in modulating pain transmission (Delfini et al., 2013; Seal et al., 2009). These fibers, whose cell bodies are located within dorsal root ganglia (DRG), innervate the hairy skin and project specifically toward the innermost layer of lamina II (lamina III) of the spinal cord to synapse with second-order neurons (Li et al., 2011; Lumpkin et al., 2010). Previous studies have demonstrated that C-LTMRs constitute a unique neuronal population among the DRG neurons, specifically expressing vesicular glutamate transporter 3 (VGLUT3; Seal et al., 2009) and TFAA4, a chemokine-like secreted protein (Delfini et al., 2013). In a persistent pain model, TFAA4 null mice developed mechanical hypersensitivity, which was reversed by an intrathecal injection of TFAA4 (Delfini et al., 2013). Although potassium channels were identified as a putative target of TFAA4, the mechanisms underlying the control of sensori-nociceptive integration by TFAA4 remains poorly understood. Surprisingly, TFAA4 was recently identified as a ligand of formyl peptide receptor 1 (FPR1) that is expressed both on macrophages (Wang et al., 2015), where it promotes cell migration and phagocytosis, and on microglial cells (Gavins, 2010).

In this study, we used the C-LTMRs' restricted expression of TFAA4 to investigate the contribution of these neurons to the control of nociceptive information transmission. We demonstrate by whole-cell recordings of lamina III neurons that application of TFAA4 induces an increase in inhibitory synaptic activity through presynaptic mechanisms, which, in turn, dampens



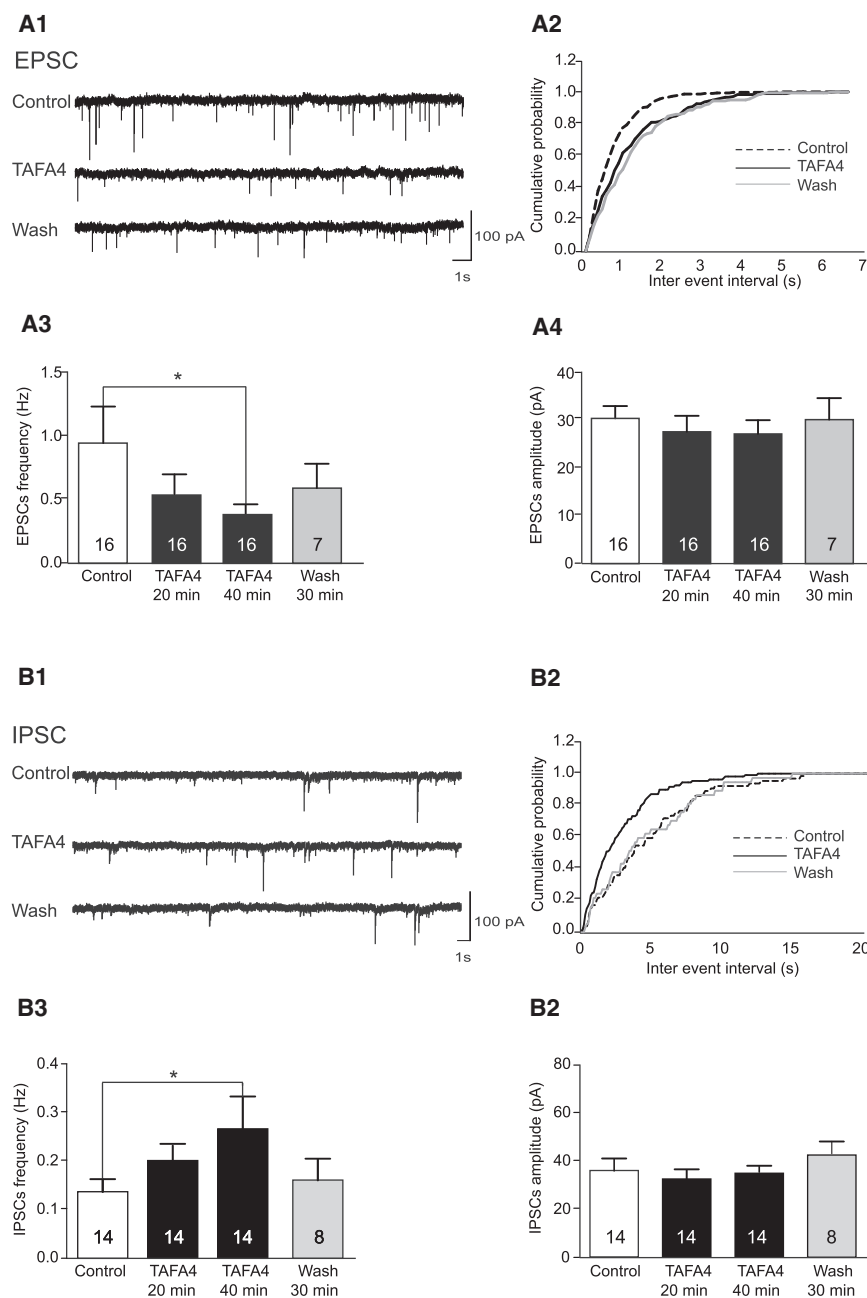


**Figure 1. Effects of TAF4 on Spontaneous Synaptic Activity of Lamina III Neurons**

(A and B) Shown in (A1) and (B1): representative current traces of EPSCs (A1) and IPSCs (B1) recorded from lamina III neuron in control, after 40 min of TAF4 superfusion, and after washout. (A2 and B2) Cumulative distribution of inter-EPSC (A2) and IPSC (B2) intervals corresponding to traces in (A1) and (B1) (control versus TAF4:  $p < 0.05$ , Kolmogorov-Smirnov test). (A3 and A4) Quantification of EPSC mean frequency (A3) and amplitude (A4) in control ( $n = 16$ ), following 20 and 40 min TAF4 superfusion ( $n = 16$ ), and after washout ( $n = 7$ ). (B3 and B4) Quantification of IPSC mean frequency (B3) and IPSC amplitude (B4) in control ( $n = 14$ ), following 20-min and 40-min TAF4 superfusion ( $n = 14$ ), and after washout ( $n = 8$ ). Data are represented as mean  $\pm$  SEM. \* $p < 0.05$ , repeated-measures ANOVA for (A3), (A4), (B3), and (B4).

microglia in TAF4-induced inhibition, we demonstrate that TAF4 loses its effect on spontaneous synaptic activity when the activation of microglial cells is prevented. TAF4 also induces microglial retraction, which enables the specific restoration of inhibitory synapses on lamina III neurons, thus promoting the reinforcement of inhibitory transmission. Altogether, these results highlight a close interplay between sensory neurons, microglial cells, and local spinal neurons, leading to the fine-tuning of inhibitory activity and nociceptive transmission in pathological conditions.

## RESULTS

### TAF4 Modulates Spontaneous and Evoked Synaptic Transmission in Dorsal Spinal Cord through Presynaptic Mechanisms

To gain further understanding of the effects of TAF4 on synaptic transmission within the spinal cord, we recorded spontaneous synaptic events in Rexed lamina III neurons using whole-cell patch-clamp recordings (Figure 1A1, top) and assessed the effects of TAF4 superfusion on the frequency and amplitude of these events. Bath application of TAF4 (20 nM) induced a significant decrease in spontaneous excitatory post-synaptic current (EPSC) event frequency (Figure 1A1, middle), as indicated by the shift in the interval cumulative distribution curve toward the left (Figure 1A2, same cell as in Figure 1A1;  $n = 10$  out of 16). This effect was long lasting, as only 2 cells out of 7 showed a significant recovery upon washout. Although this decrease could be observed 20 min after the onset of TAF4 superfusion, it became significant only after 40 min (Figure 1A3). All in all, the

excitatory synaptic transmission and impairs transmission between nociceptive fibers and interneurons. In CFA (complete Freund's adjuvant)-inflamed animals, TAF4 induces a decrease in the neuronal activity evoked by noxious stimulation of the hindpaw that is dependent on GABAergic transmission integrity. Furthermore, intrathecal administration of TAF4 provides analgesic effects that are also blocked by GABA receptor antagonists, so GABAergic interneurons are the first relay in the integration of information transmitted by C-LTMRs. Interestingly, ultrastructural studies revealed close interaction between TAF4-expressing primary afferent fibers (PAFs) and GABAergic terminals in lamina III. By investigating the role of

excitatory synaptic events in Rexed lamina III neurons using whole-cell patch-clamp recordings (Figure 1A1, top) and assessed the effects of TAF4 superfusion on the frequency and amplitude of these events. Bath application of TAF4 (20 nM) induced a significant decrease in spontaneous excitatory post-synaptic current (EPSC) event frequency (Figure 1A1, middle), as indicated by the shift in the interval cumulative distribution curve toward the left (Figure 1A2, same cell as in Figure 1A1;  $n = 10$  out of 16). This effect was long lasting, as only 2 cells out of 7 showed a significant recovery upon washout. Although this decrease could be observed 20 min after the onset of TAF4 superfusion, it became significant only after 40 min (Figure 1A3). All in all, the

average frequency of EPSCs was 59.5% lower in the presence of TAF4 than in control conditions (control:  $0.94 \pm 0.29$  Hz,  $n = 16$ ; TAF4, 20 min:  $0.540 \pm 0.16$  Hz,  $n = 16$ ; TAF4, 40 min:  $0.382 \pm 0.08$  Hz,  $n = 16$ ; wash:  $0.587 \pm 0.19$  Hz,  $n = 7$ ;  $p < 0.05$ ). The distribution of EPSC decay was similar in control and TAF4 conditions (Figure S1A,  $n = 16$ ). Strikingly, the amplitude of EPSCs was not affected by TAF4 superfusion (Figure 1A4; control:  $30.83 \pm 2.88$  pA; TAF4, 20 min:  $27.12 \pm 3.2$  pA; TAF4, 40 min:  $27.46 \pm 4.54$  pA; wash:  $29.98 \pm 3.0$  pA), suggesting the involvement of a pre-synaptic mechanism.

By contrast, the frequency of spontaneous inhibitory postsynaptic currents (IPSCs) recorded using a chloride-enriched solution (Figure 1B1, top) exhibited a dramatic increase following TAF4 superfusion, as indicated by the shift toward the right of the inter-event interval cumulative distribution curve (Figures 1B1, middle, and 1B2;  $n = 10$  out of 14; Figures 1B1 and 1B2 are of the same cell). This increase was reversed upon rinsing in 3 cells out of 8. The distribution of IPSC decay was similar in control and TAF4 conditions (Figure S1B,  $n = 8$ ). On average, after 40 min of application, TAF4 induced a 94% increase in IPSC frequency (Figure 1B3; control:  $0.14 \pm 0.026$  Hz,  $n = 14$ ; TAF4, 20 min:  $0.20 \pm 0.03$  Hz,  $n = 14$ ; TAF4, 40 min:  $0.27 \pm 0.06$  Hz,  $n = 14$ ; wash:  $0.16 \pm 0.02$  Hz,  $n = 8$ ;  $p < 0.05$ ) without affecting IPSC average amplitude (Figure 1B4; control:  $35.00 \pm 5.51$  pA; TAF4, 20 min:  $31.98 \pm 3.77$  pA; TAF4, 40 min:  $34.16 \pm 3.19$  pA; wash:  $41.90 \pm 5.91$  pA), thereby reinforcing the hypothesis of a pre-synaptic action of TAF4.

To show that the effects of TAF4 on EPSC and IPSC frequency were mediated by pre-synaptic mechanisms, we monitored the frequency of miniature synaptic events (mEPSC and mIPSC) in the presence of tetrodotoxin (TTX) to block action potential propagation in control, following 40 min of TAF4 application and after washout (Figure 2A1). In the presence of TTX, TAF4 induced a significant decrease in mEPSC frequency in 6 out of 14 neurons (Figure 2A2). On average, mEPSC frequency was 32% lower following TAF4 exposure than in control conditions (Figure 2A3; control:  $0.35 \pm 0.091$  Hz; TAF4, 40 min:  $0.24 \pm 0.06$  Hz;  $p < 0.05$ ). On the other hand, TAF4 induced a significant increase in mIPSC frequency recorded in the presence of TTX in 6 cells out of 8 (Figures 2B1 and 2B2). On average, the frequency of mIPSCs was 169% higher under TAF4 superfusion than in control conditions (Figure 2B3; control:  $0.09 \pm 0.01$  Hz; TAF4, 40 min:  $0.23 \pm 0.04$  Hz; wash:  $0.18 \pm 0.07$  Hz;  $p < 0.05$ ). Under TTX superfusion, TAF4 had no effect on mEPSC or mIPSC amplitude (data not shown). Therefore, the effects of TAF4 on EPSC and IPSC frequencies were preserved in the presence of TTX, indicating a presynaptic regulation of synaptic transmission.

To investigate whether TAF4 also presynaptically modulates synaptic transmission between high-threshold PAF and lamina III neurons, we recorded in lamina III the synaptic responses evoked by paired maximal stimulations of attached dorsal roots (Figures 2C1 and 2C2). Following TAF4 application, the amplitude of the first evoked EPSC was greatly reduced (Figure 2C3;  $n = 18$ ; average:  $-35\%$ ; control:  $-347 \pm 94$  pA; TAF4:  $-225 \pm 60$  pA;  $p < 0.05$ ), while the paired pulse ratio (PPR) of the synaptic responses was significantly increased (Figure 2C4;  $n = 18$ ; average:  $+28.8\%$ ; control:  $0.81 \pm 0.10$ ; TAF4:  $1.046 \pm 0.12$ ),

Thus, TAF4 impairs synaptic transmission between PAFs and lamina III neurons by decreasing neurotransmitter release from high-threshold presynaptic sensory fibers.

### TAF4 Modulates Excitatory Transmission through GABA Receptors

The decrease in EPSC frequency and synaptic transmission between primary fibers and lamina III neurons could result from an increased inhibitory tonus exerted on excitatory neurons and primary fibers. To test this hypothesis, we recorded EPSC frequency while blocking inhibitory transmission (Figure 3A1) with CGP55845A (CGP) and bicuculline (antagonists of GABA<sub>B</sub> and GABA<sub>A</sub> receptors, respectively) and with strychnine (antagonist of glycinergic receptors). We found no difference in the average EPSC frequency between control and TAF4 conditions (Figure 3A2;  $n = 10$ ; control:  $2.80 \pm 1.04$  Hz; TAF4:  $2.16 \pm 0.61$  Hz), indicating that the effect of TAF4 on EPSC frequency is dependent upon inhibitory transmission. Of note, TAF4 had no effect on mEPSC frequency when inhibitory transmission was blocked (Figure S2). More specifically, by blocking solely GABAergic or glycinergic transmission, we found that TAF4 no longer modulated EPSC frequency when GABAergic transmission alone was blocked (Figure 3A3;  $n = 11$ ; control:  $0.63 \pm 0.32$  Hz; TAF4:  $0.80 \pm 0.42$  Hz), whereas a decrease in EPSC frequency was still observed upon TAF4 application when only glycinergic transmission was blocked (Figure 3A4;  $n = 17$ ; control:  $0.50 \pm 0.15$  Hz; TAF4:  $0.35 \pm 0.09$  Hz;  $p < 0.05$ ).

Similarly, the addition of CGP and bicuculline to the perfusion medium blocked the effects of TAF4 on the amplitude (Figures 3C1 and 3C2;  $n = 15$ ; average:  $-5.3\%$ ; control:  $-431 \pm 112$  pA; TAF4:  $-408 \pm 117$  pA; compare with Figure 2C3) and the PPR (Figures 3C1 and 3C3;  $n = 15$ ; average:  $-1.4\%$ ; control:  $0.86 \pm 0.08$ ; TAF4:  $0.86 \pm 0.12$ ; compare with Figure 2C4) of dorsal-root-evoked synaptic responses. Thus, the TAF4-mediated decrease in EPSC frequency and in synaptic transmission between PAFs and spinal interneurons is indirect and mainly mediated by a modulation of GABAergic transmission by TAF4.

### C-LTMRs Make Direct Contact onto GABAergic Neurons

There is, therefore, a close functional interaction between TAF4 and inhibitory GABAergic transmission. As C-LTMRs are the only source of TAF4 within the spinal cord (Delfini et al., 2013), we investigated whether direct contact between C-LTMR fibers and GABAergic neurons could be observed in the spinal cord. We used TAF4<sup>Venus</sup> knockin mice (Delfini et al., 2013) to perform multiple immunolabeling ultrastructural experiments and used GFP and VGLUT3 as markers of C-LTMRs and IB4 as a marker of non-peptidergic PAFs. Venus was specifically co-expressed with VGLUT3 in a population of non-peptidergic PAFs but was not present in IB4-immunolabeled fibers (Figure 4A). The central terminal of Venus-positive fibers formed typical type 1a glomeruli with an electron-dense C bouton filled by small agranular synaptic vesicles surrounded by numerous dendrites (indicated with a "d" in Figure 4A), including a presynaptic-vesicle-containing dendrite (V1) and a few peripheral axons (V2; data not shown; see also Figure S5). Venus-positive fibers mostly formed contacts with GABA-IR presynaptic vesicle-containing dendrites

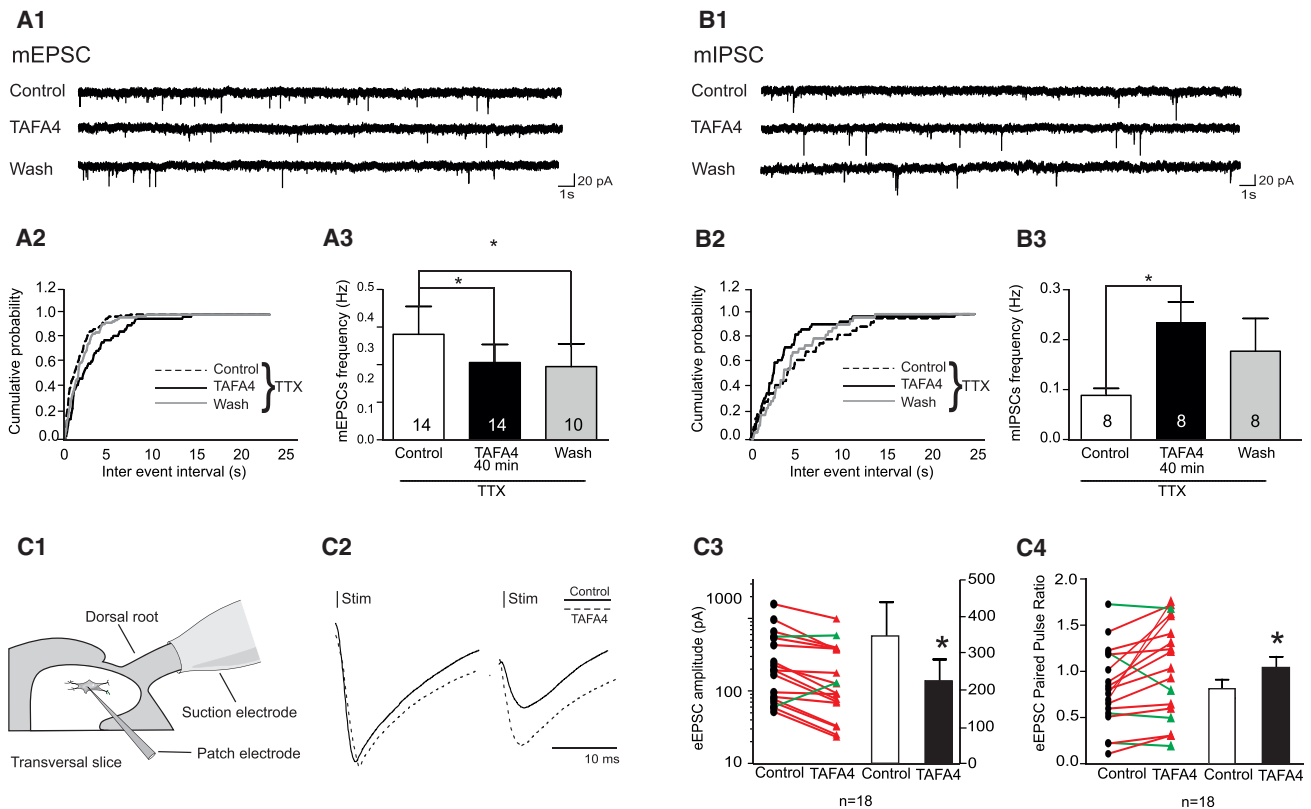


**Figure 2. Presynaptic Action of TAF4 on Spontaneous and Evoked Synaptic Activity**

(A and B) Shown in (A1) and (B1): representative current traces of miniature EPSCs (A1) and IPSCs (B1) recorded from a lamina III neuron under TTX in the control condition, following 40 min of TAF4 superfusion, and after wash. (A2 and B2) Cumulative distribution of inter-mEPSC (A2) and mIPSC (B2) intervals corresponding to traces in (A1) and (B1) (control versus TAF4:  $p < 0.05$ , Kolmogorov-Smirnov test). (A3 and B3) Quantifications of lamina III neuron mEPSC (A3) and mIPSC (B3) mean frequencies (mEPSC:  $n = 14$ ; mIPSC:  $n = 8$ ) following 40-min TAF4 superfusion (mEPSC:  $n = 14$ ; mIPSC:  $n = 8$ ) and after washout (mEPSC:  $n = 14$ ; mIPSC:  $n = 8$ ).

(C) Shown in (C1): schematic representation of experimental procedure used to record evoked EPSCs from lamina III neurons. (C2) Normalized representative traces of evoked EPSCs obtained before and after bath application of TAF4. (C3 and C4) Quantification of the amplitude of the first evoked EPSC (C3;  $n = 18$ ) and PPR of synaptic responses in control and TAF4 conditions (C4;  $n = 18$ ). Decreases in synaptic responses and increases in PPR are presented in red, while increases in synaptic response and decreases in PPR are represented in green.

\* $p < 0.05$ , one-way repeated-measures ANOVA for (A3) and (B3), Wilcoxon signed-rank test for (C3), and Student's paired t test for (C4). ns, not significant.

(V1 in Figure 4B). After quantitative analysis of 150 GFP-IR-Gla ( $N = 3$  mice), we observed that all V1 were GABA immunolabeled, only a minority of V2 were GABA-IR, while no plain dendrites (d in Figure 4C) were GABA-IR. These data showed a net predominance of synaptic contacts between GFP-positive fibers and GABA-IR V1 (95.9%; Figure 4D) rather than GABA-IR V2 (4.1%; Figure 4D). Hence, C-LTMR fibers establish direct synaptic contact with GABAergic interneurons within lamina III.

### TAF4 Alleviates CFA-Induced Pain through Reinforcement of Inhibitions within Spinal Cord

Our patch-clamp experiments demonstrated that TAF4 increases inhibitory transmission within the spinal cord, which, in turn, depresses excitatory transmission, including transmission between high-threshold PAFs and spinal interneurons. To assess whether this mechanism may account for the antinociceptive effects of TAF4, we used an inflammatory pain model consisting of an injection of CFA in the rear paw.

Four days after CFA injection, we performed whole-cell patch-clamp recordings on spinal cord slices incubated for 40 min in TAF4 or in artificial cerebro spinal fluid (aCSF). Slices incubated in TAF4 exhibited lower average EPSC frequency (Figure S3A) and higher average IPSC frequency (Figure S3B) than slices incubated in aCSF. The average PPR of synaptic responses evoked by dorsal root stimulation was also higher in slices incubated in TAF4 (Figure S3C). Altogether, these data suggest that the mechanisms identified in spinal slices of naive animals are mostly conserved in slices of CFA animals.

We next used extracellular *in vivo* recordings of superficial spinal cord neurons to assess the effects of TAF4 on the neuronal discharge evoked by Von Frey hair noxious stimulation of the hindpaw. In naive animals, intraspinal injection of TAF4 or aCSF had no effect on the average discharge frequency of neurons during hindpaw stimulation (Figures S4A and S4B). By contrast, in CFA-inflamed animals, TAF4 induced a significant decrease in the neuronal discharge following a noxious stimulus

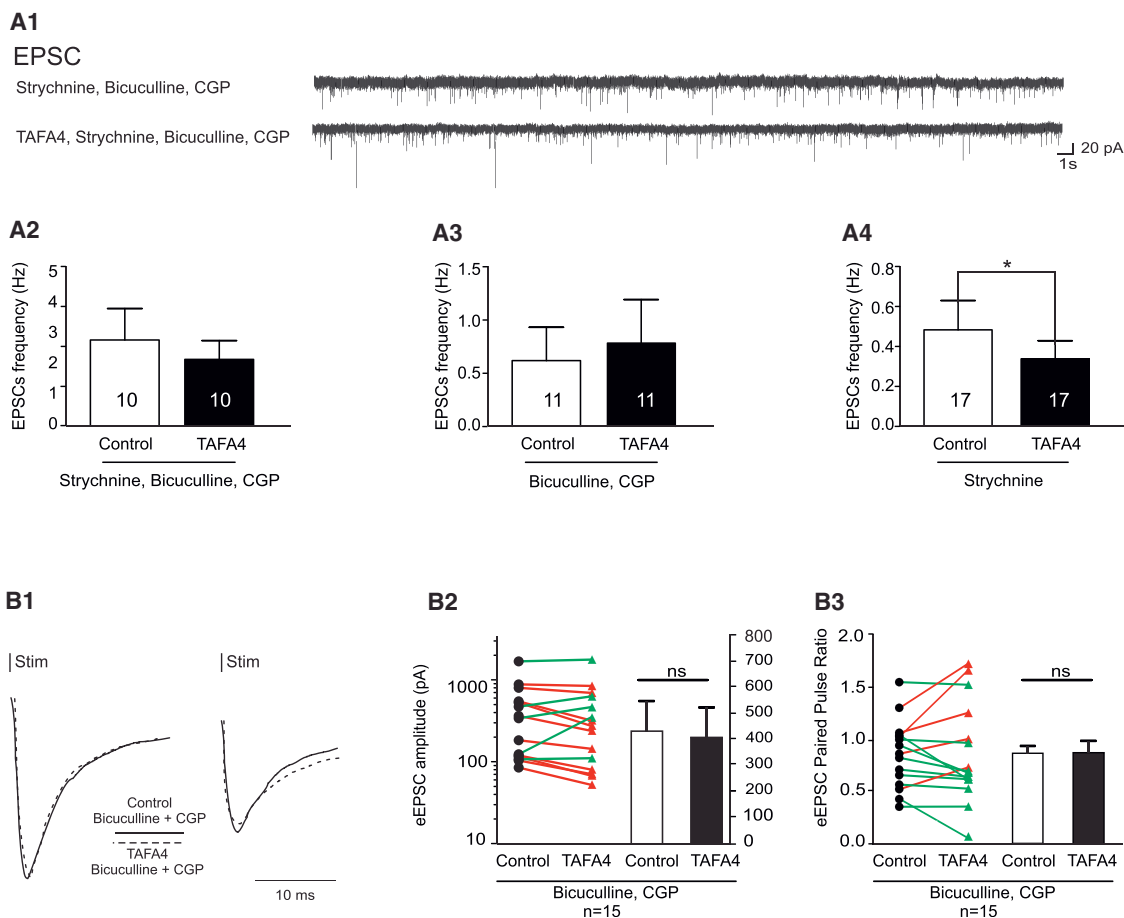


**Figure 3. The Effect of TAF4 on Excitatory Transmission Is Mediated by Inhibitory Transmission**

(A) Shown in (A1): representative traces of EPSCs recorded with antagonists of GABA<sub>A</sub> (bicuculline), GABA<sub>B</sub> (CGP), and glycinergic receptors (Strychnine), before and after 40 min of exogenous application of TAF4. (A2–A4) Histogram comparing EPSC frequency before and after application of TAF4 in the presence of bicuculline, CGP, and strychnine (A2; n = 10); bicuculline and CGP only (A3; n = 11); or strychnine only (A4; n = 17).

(B) Shown in (B1): normalized representative traces of evoked excitatory synaptic responses obtained before and after bath application of TAF4 in the presence of bicuculline and CGP. (B2 and B3) Quantification of amplitude of the first evoked EPSC (B2; n = 15) and PPR of synaptic responses in the control and TAF4 conditions (B3; n = 15). Decreases in synaptic responses and increases in PPR are presented in red, while increases in synaptic response and decreases in PPR are represented in green.

Data are represented as mean ± SEM. \*p < 0.05, paired Student's t test for (A2)–(A4), Wilcoxon signed-rank test for (B2), and Student's paired t test for (B3). ns, not significant.

(Figures 5A1 and 5A2; N = 5; control: 152.39 ± 16.08 Hz; TAF4, 40 min: 109.55 ± 29.50 Hz; p < 0.05) that was not observed when aCSF only was injected (Figures 5A1 and 5A2; N = 5; control: 93.70 ± 22.89 Hz; TAF4, 40 min: 128.41 ± 31.59 Hz). Furthermore, this decrease was abolished when TAF4 was co-injected with blockers of GABAergic synaptic transmission (Figures 5B1 and 5B2; N = 5; control: 70.33 ± 5.06 Hz; TAF4, 40 min: 76.36 ± 4.47 Hz). Taken together, these results demonstrate that TAF4 impaired the integration of noxious input through GABAergic transmission in inflammatory conditions.

Finally, we investigated whether mechanical hypersensitivity developed by CFA-inflamed animals could be reversed with an intrathecal injection of TAF4 and whether this reversal was dependent upon GABAergic transmission. Von Frey tests performed 4 days after CFA injection showed that inflamed animals

exhibited a dramatic decrease in paw withdrawal threshold that could be partially reversed within 1 hr following an intrathecal injection of TAF4 (Figure 5C; N = 16; control: 1.12 ± 0.13 g; CFA: 0.09 ± 0.03 g; CFA-TAF4: 0.50 ± 0.06 g; p < 0.05). However, no reversal of pain threshold was observed when TAF4 was co-injected with antagonists of the GABA<sub>A</sub> and GABA<sub>B</sub> receptors bicuculline and phaclofen, respectively (Figure 5C; N = 12; 0.057 ± 0.006 g), indicating that the antinociceptive effect of TAF4 is mediated by GABAergic transmission.

#### TAF4 Induces Microglial Retraction in CFA Animals

A recent study (Wang et al., 2015) demonstrated that TAF4 binds FPR1 expressed on macrophages and microglial cells. To assess whether microglia are involved in the modulation of inhibitory transmission mediated by TAF4, we first recorded

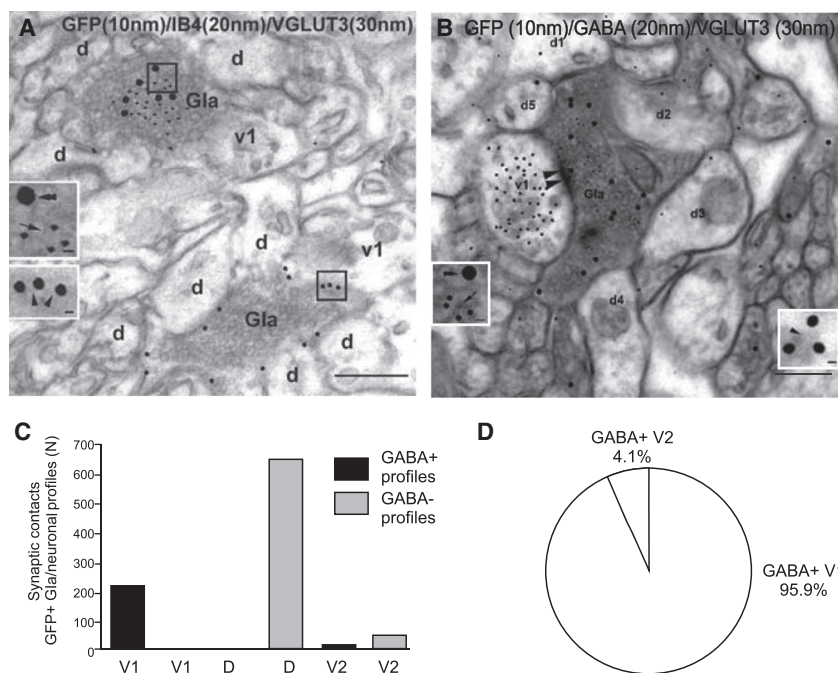


**Figure 4. Ultrastructural Localization of TAF4-Expressing C-LTMRs and Relationship with Lamina III GABA-IR Interneurons**

(A) Two immunoreactive type Ia non-peptidergic glomeruli (Gla) in lamina III. The Gla at top in the figure is double-labeled for GFP (10-nm gold particles; in the top left insert, this is indicated with an arrow) and VGLUT3 (30-nm gold particles; in the top left insert, this is indicated with a double arrowhead), while the Gla at bottom is labeled only for IB4 (20-nm gold particles; in the bottom left insert, this is indicated with arrowheads). GFP and VGLUT3 are scattered over the Gla central terminal, while IB4 is exclusively localized over the Gla plasma membrane. Scale bars, 300 nm; 20 nm in the inserts.

(B) A GFP + VGLUT3-immunoreactive Gla is surrounded by different unlabeled dendrites (d) and makes a synapse with a GABA-immunolabeled vesicle-containing dendrite (V1 [indicated as v1], arrowheads). GFP (10-nm gold particles) and VGLUT3 (30-nm gold particles) are scattered over the Gla central terminal (left insert; indicated with an arrow and a double arrowhead, respectively). GABA (20-nm gold particles) is distributed in the intracellular aspect of the V1 (indicated with an arrowhead in the right insert). Scale bars: 300 nm; 20 nm in inserts.

(C) Histogram showing the number of synaptic contacts between GFP-immunolabeled Gla and the

surrounding neuronal profiles (V1, vesicle-containing dendrites; D, plain dendrites; V2, peripheral axons) engaged in the glomerular configuration (black bars indicate number of synaptic contacts between GFP-IR Gla/GABA-positive V1 and V2 profiles; gray bars indicate number of synaptic contacts between GFP-IR Gla/GABA-negative D and V2 profiles). Quantitative analysis was performed by observing randomly selected images of GFP-immunolabeled Gla ( $n = 150$  from  $N = 3$  mice) at a magnification of  $40,000\times$  to precisely identify the synaptic contacts.

(D) Pie chart showing the percentage of synaptic contacts between GFP+ Glu/GABA-IR V1 (95.9%) and GFP+ Glu/GABA-IR V2 (4.1%). Quantitative analysis was performed by observing the same randomly selected images of GFP-immunolabeled Gla ( $n = 150$  from  $N = 3$  mice) used for the analysis described in (C).

EPSCs and IPSCs in spinal cord slices pre-incubated with minocycline, which inhibits microglial activation. After TAF4A superfusion, no significant changes were detected either in EPSC frequency (Figures 6A1 and 6A2;  $n = 10$ ; control:  $0.38 \pm 0.15$  Hz; TAF4A:  $0.35 \pm 0.18$  Hz) or IPSC frequency (Figures 6B1 and 6B2;  $n = 10$ ; control:  $0.26 \pm 0.10$  Hz; TAF4A:  $0.12 \pm 0.04$  Hz) when the activation of microglia was inhibited. Thus, microglia are required for TAF4A to induce a shift in inhibitory/excitatory balance (compare Figure 1A3 with Figure 6A2 and Figure 1B3 with Figure 6B2).

We then characterized microglial reactivity in the dorsal horn of inflamed animals treated or not treated with TAF4A by using immunohistochemistry to quantify the surface labeled by the ionized calcium binding adaptor molecule 1 (Iba1; Figure 6C1). CFA injection induced a significant increase in the surface labeled by Iba1 that was partially reversed by the intrathecal injection of TAF4A (Figure 6C2;  $N = 3$ ; naive:  $1.55 \pm 0.31\%$ ; CFA:  $6.99 \pm 0.27\%$ ; CFA + TAF4A:  $5.39 \pm 0.27\%$ ;  $p < 0.05$ ), showing that TAF4A reduces microglial activation. Strikingly, our electron microscopy (EM) data suggest that putative microglial cells may contact GABAergic V1 profiles surrounding C-LTMRs endings (Figure S5). To investigate whether the interaction between microglial cells and inhibitory synapses is altered by TAF4A, we performed immunohistochemistry to label gephyrin, a specific post-synaptic marker of inhibitory synapses, and Iba1 and quantified the number of inhibitory synapses in close apposition with microglial cells. Strikingly, the spreading of microglia in the

dorsal horn of CFA animals was accompanied by an increase in the number of inhibitory synapses in contact with microglial cells (yellow dots). Furthermore, this increase was partially reversed following intrathecal TAF4A injection (Figures 6D1 and 6D2;  $N = 3$ ; control:  $1.76 \pm 0.40\%$ ; CFA:  $5.31 \pm 0.20\%$ ; CFA + TAF4A:  $3.52 \pm 0.43\%$ ;  $p < 0.05$ ). Altogether, our data provide evidence that TAF4A reverses the increased interaction between inhibitory synapses and microglial processes observed in inflammatory conditions. Furthermore, by quantifying the surface of neuronal soma (revealed by immunodetection of NeuN) occupied by inhibitory synapses (labeled by gephyrin; Figure 7A1), we found that CFA inflammation induced a reduction in the soma surface co-labeled with gephyrin compared to naive animals, suggesting a disruption of inhibitory synapses in CFA animals. In TAF4A-treated inflamed mice, the surface of neuronal somata occupied by inhibitory synapses was recovered and similar to the control level, indicating a restoration of inhibitory contacts on lamina III somata (Figure 7A2; 315 neurons from  $N = 3$  animals; control:  $4.96 \pm 0.50\%$ ; CFA:  $3.66 \pm 0.33\%$ ; CFA + TAF4A:  $5.26 \pm 0.52\%$ ;  $p < 0.05$ ). Remarkably, similar experiments quantifying the number of excitatory synapses labeled with the post-synaptic excitatory synapse marker Homer (Figure 7B1) revealed no difference in the neuron soma area covered by excitatory synapses between naive animals, CFA-inflamed animals, and CFA-inflamed animals treated with TAF4A (Figure 7B2; 315 neurons from  $N = 3$  animals; control:  $12.43 \pm 1.75\%$ ; CFA:  $12.48 \pm 1.05\%$ ; CFA + TAF4A:  $13.29 \pm 1.04\%$ ).

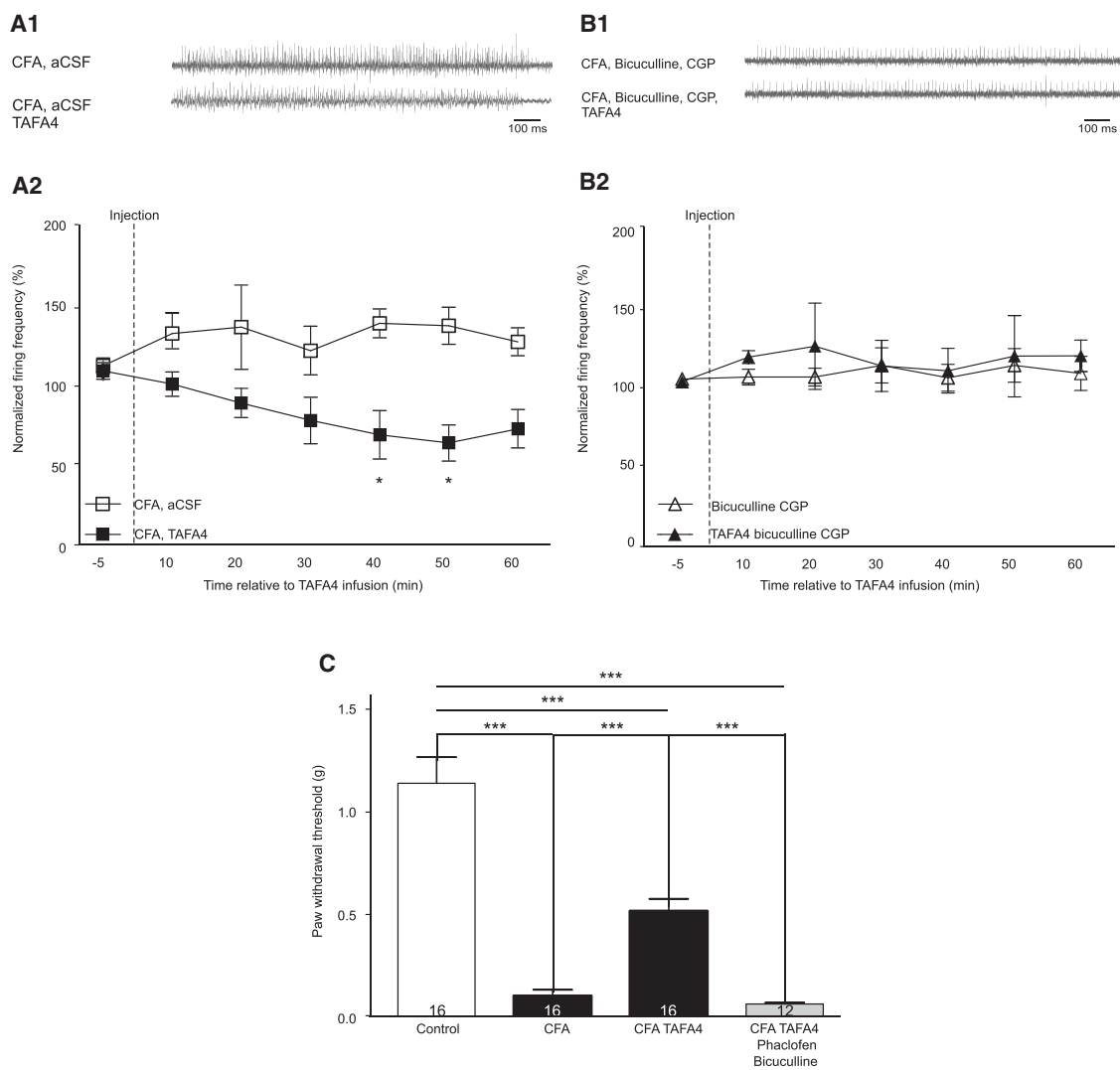


**Figure 5. TFAFA4 Decreases Neuronal Discharge Elicited by Noxious Stimulation in CFA Animals**

(A) Shown in (A1): representative traces of extracellular *in vivo* recordings obtained from neurons located in superficial laminae activated by a noxious mechanical stimulus (Von Frey hair filament, 15 g) in CFA animals after an infusion of either aCSF or TFAFA4. (A2) Quantification of action potential mean frequency measured in control condition (−5 min) and every 10 min after injection of aCSF (N = 5) or TFAFA4 (N = 5) until 60 min.

(B) Shown in (B1): representative neuronal responses to a mechanical noxious stimulus recorded with antagonists of GABA<sub>A</sub> and GABA<sub>B</sub> receptors (bicuculline and CGP) co-injected with either aCSF or TFAFA4. (B2) Quantification of action potential frequency before and after intra-spinal injection of aCSF or TFAFA4 in the presence of GABA<sub>A</sub> and GABA<sub>B</sub> antagonists (N = 5).

(C) Histogram of mechanical sensitivity assessed with Von Frey hairs in naive (N = 16) or CFA (N = 16) animals intrathecally injected with TFAFA4 (N = 16) and TFAFA4 with phaclofen and bicuculline (N = 12).

Data are represented as mean ± SEM. \*p < 0.05; \*\*\*p < 0.001, two-way repeated-measures ANOVA followed by Newman-Keuls test for (A2) and (B2) and Student's t test for (C).

Altogether, our experiments highlight a tight interplay between the C-LTMR-derived chemokine TFAFA4, microglial cells, and inhibitory synapses. In CFA-inflamed animals, microglial spreading promotes the synaptic stripping of inhibitory synapses, resulting in a weakened inhibitory tone within spinal cord nociceptive networks. This weakened tone, in turn, reinforces both excitatory influences from local interneurons and excitatory transmission between high-threshold nociceptive fibers and lamina Ili networks (Figure 7C1). C-LTMR-derived TFAFA4 che-

mokine is able to partially reverse this microglial spreading, promoting the re-innervation of lamina Ili somata by inhibitory synapses and a reinforcement of inhibitory tone that attenuates pain transmission within the spinal cord (Figure 7C2).

## DISCUSSION

Recent findings have highlighted the role of C-LTMRs in fine-tuning pain transmission within spinal cord networks (Delfini



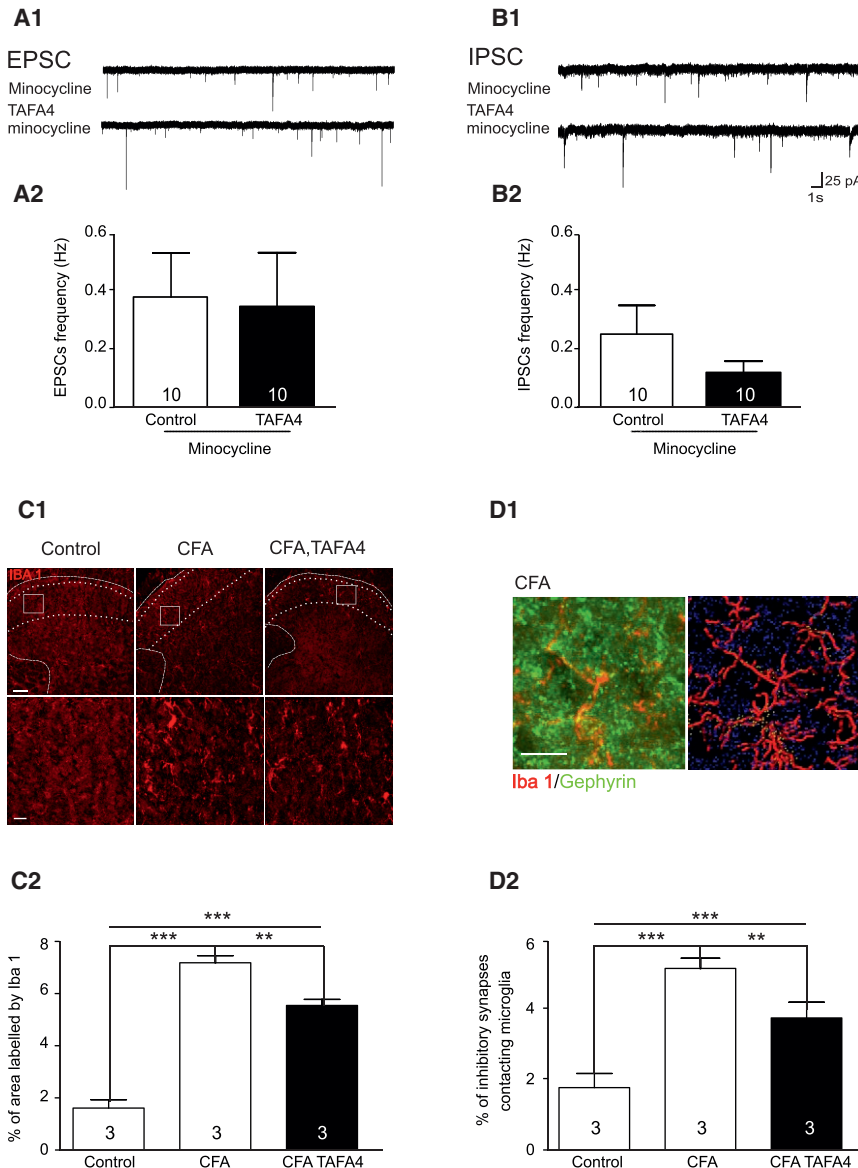


**Figure 6. The Effect of TFAFA4 Is Mediated by Microglia, which Undergo Process Retraction upon TFAFA4 Application**

(A) Shown in (A1): representative current traces of EPSCs recorded in lamina III neurons before and after TFAFA4 superfusion, in slices incubated within minocycline 1.5 hr before recording. (A2) Comparison of EPSC mean frequencies recorded in the control condition (minocycline; n = 10) and TFAFA4 condition (minocycline + TFAFA4; n = 10).

(B) Shown in (B1): representative recording of IPSCs obtained from lamina III neurons recorded in slices incubated with minocycline, before and 40 min after TFAFA4 superfusion. (B2) Quantification of IPSC mean frequencies before and after superfusion with TFAFA4 in minocycline-incubated slices (n = 10).

(C) Shown in (C1): immunohistochemistry for Iba1 in lumbar dorsal spinal cord sections (top; scale bar: 60  $\mu$ m) and in lamina III (bottom; scale bar: 20  $\mu$ m) in control, CFA-inflamed, and CFA-inflamed with intrathecal TFAFA4 animals. (C2) Quantification of the lamina II surface labeled with Iba1 (percentage of total surface of confocal acquisition) in control, inflamed, and TFAFA4-injected inflamed animals (N = 3 each).

(D) Shown in (D1): immunohistochemistry for Iba1 (red) and gephyrin (green) in lumbar spinal cord section (left panel, CFA mouse) and 3D reconstruction of immunostaining (right panel) allowing the quantification of colocalization between inhibitory synapses and microglial cells (yellow dots). (D2) Quantification of colocalization between gephyrin and Iba1 within lamina II in naive, inflamed, and TFAFA4-injected animals (N = 3 each).

Data are represented as mean  $\pm$  SEM. \*\*p < 0.01; \*\*\*p < 0.001, Student's paired t test for (A2) and (B2) and one-way ANOVA for (C2) and (D2).

**Low-Threshold Fibers and Nociceptive Pathways**

The integration of multiple sensory modalities within the dorsal spinal cord may create interferences and crosstalk between these modalities and alter the

et al., 2013; Seal et al., 2009). However, the microcircuits involved in this modulation remain poorly understood. Here, we report that C-LTMRs directly contact GABAergic interneurons in Rexed lamina III of the spinal cord. We demonstrate that C-LTMR-derived chemokine TFAFA4 increases synaptic inhibitory tone in the spinal cord, which, in turn, decreases spontaneous excitatory transmission through the recruitment of GABA receptors and weakens the transmission between PAFs and spinal interneurons, thus resulting in pain alleviation. Finally, we demonstrate that TFAFA4 reverses CFA-induced microglial extension and promotes an increase in the density of inhibitory synapses on lamina III neurons. Altogether, our results suggest that C-LTMRs promote the retraction of microglial processes by releasing TFAFA4 in the vicinity of inhibitory neurons, thus enabling the restoration of inhibitory synapses within lamina III.

transmission of sensory stimuli (Craig and Bushnell, 1994; Mackenzie et al., 1975; Yarnitsky and Ochoa, 1990).

For instance, in pathological pain, low-threshold fibers involved in touch transmission elicit pain by activating superficial dorsal horn networks dedicated to the integration of noxious stimuli (Baba et al., 2003; Daniele and MacDermott, 2009; Mirau-court et al., 2007). On the contrary, low-frequency stimulation of low-threshold fibers ( $A\beta$ ) may alleviate pain by inducing synaptic depression in *substantia gelatinosa* neurons (Sdrulla et al., 2015). Although recent studies have deciphered neuronal microcircuits through which touch neurons may alleviate pain transmission (Duan et al., 2014; Lu et al., 2013), the spinal circuitry underlying this alleviation remains poorly understood. In our study, we demonstrate that C-LTMRs contact GABAergic interneurons. Given the findings of Lu and Perl (2005), who demonstrated that islet cells receive non-noxious C-fiber inputs, and of

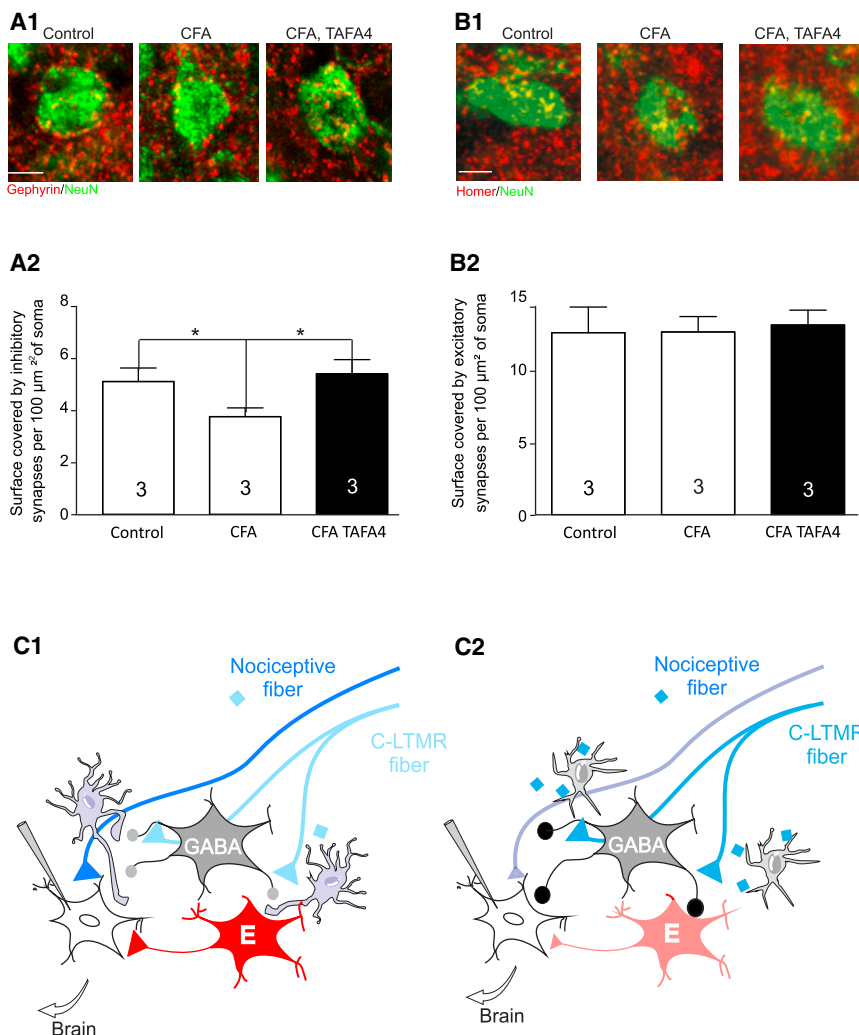


**Figure 7. Restoration of Inhibitory Contacts on Dorsal Spinal Cord Neurons by TAF A4**

(A1 and B1) High-magnification images of a lamina II neuronal soma immunolabeled for NeuN and surrounding inhibitory (A1, labeled with gephyrin) and excitatory (B1, labeled with Homer) synapses in control, CFA, and TAF A4-injected CFA animals. (A2 and B2) Quantifications of neuronal soma surface occupied by (A2) gephyrin or (B2) Homer in control, CFA, and CFA TAF A4-injected (n = 315 neurons from N = 3 animals each) animals. Scale bars, 10 μm.

(C) Schematic representation of the proposed mechanism of action of TAF A4. (C1) In the inflammatory condition, activated microglia displace inhibitory synapses from neuronal soma, leading to an increase in excitatory transmission and, thus, a CFA-induced hypersensitivity. (C2) By inducing a reduction in microglial spreading, TAF A4 promotes the partial restoration of inhibitory transmission. Data are represented as mean ± SEM. \*p < 0.05, one-way ANOVA for (C2) and (D2).

previous studies showing that GABA<sup>+</sup> V1 profiles in the GlA configuration belong to islet cells (Bardoni et al., 2007; Ribeiro-da-Silva, 2004), we propose that C-LTMRs synapse onto islet cells within lamina II, thus providing a direct pathway between low-threshold fibers and GABAergic neurons involved in the modulation of noxious stimuli transmission.

### The Effects of TAF A4 Are Mediated through GABAergic Transmission

Many inhibitory neurons in lamina II exhibit both GABA and glycine immunoreactivity (Polgár et al., 2013), and the co-release of both transmitters at some mixed GABAergic/glycinergic synapses has been demonstrated (Chéry and De Koninck, 1999; O'Brien and Berger, 1999). Surprisingly, we found that blocking GABAergic transmission is sufficient to prevent the effects of TAF A4, thereby suggesting the segregation of GABAergic and glycinergic inhibitory pathways. In rat spinal cord, the co-release of GABA and glycine was found to be pronounced during development and to have ceased by adulthood (Keller et al., 2001). This separation of GABAergic and glycinergic systems is in line with findings from recent studies showing segregation of glyci-

nergic and GABAergic inputs on dorsal horn excitatory neurons, depending on their dorso-ventral location (Takazawa et al., 2017). Differences can also be observed in the distribution of glycine and GABA receptors (Harvey et al., 2004; Todd et al., 1996), thus demonstrating that GABAergic and glycinergic pathways are functionally distinct in the spinal cord.

As mentioned earlier, our results, together with the findings of Lu and Perl (2005), suggest that C-LTMRs contact islet cells. The latter are all GABAergic, and only some of them seem to co-express glycine (Spike and Todd, 1992). In

addition, Lu and Perl (2005) demonstrated that the synapse between islet cells and central cells is blocked by GABA<sub>A</sub> antagonists, which reinforces our finding that the effects of TAF A4 are mediated mainly by GABAergic transmission.

We did not challenge the respective role of GABA<sub>A</sub> versus GABA<sub>B</sub> receptors in mediating the effects of TAF A4. Our previous findings (Delfini et al., 2013) identified potassium channels as putative targets for TAF A4. As potassium channels may be highly modulated by GABA<sub>B</sub> receptors, one could postulate that, in addition to GABA<sub>A</sub> receptors, GABA<sub>B</sub> receptors may also partly mediate the effects of TAF A4. Thus, by restoring GABAergic inhibition, TAF A4 could alter the intrinsic properties and the excitability of spinal interneurons through yet-unidentified signaling cascades. An action mediated by GABA<sub>B</sub> receptors involving the recruitment of signaling cascades and long-term cell plasticity could also partly explain why we rarely observed a recovery upon TAF A4 washout.

### Microglia Are Required for the Effects of TAF A4

Microglia are known to regulate the efficacy of synaptic transmission and, specifically, inhibitory transmission in pathological

pain conditions (Ji et al., 2013) through a wide range of mechanisms. For instance, in neuropathic pain models, brain-derived neurotrophic factor (BDNF) released by microglial cells within the spinal cord induces an inversion of the polarity of GABA-mediated currents and contributes to tactile allodynia after nerve injury (Coull et al., 2005). Moreover, proinflammatory cytokines such as interleukin-1 $\beta$ , interleukin-6, and tumor necrosis factor- $\alpha$  are involved in central sensitization by increasing excitatory synaptic transmission or reducing inhibitory synaptic transmission (Clark et al., 2015; Kawasaki et al., 2008). In inflammatory pain models, some studies have reported a lack of spinal microglial activation when CFA is injected in the rear paw (Lin et al., 2007; Sun et al., 2007), while others have reported clear indicators of microglial activation following CFA hindpaw inflammation (Hui et al., 2013; Liao et al., 2017; Qi et al., 2016; Raghavendra et al., 2004; Xu et al., 2014). We found that CFA induced a major increase in the surface immunostained by Iba1 within lamina II of the spinal cord. Surprisingly, intrathecal injection of TFAFA4 reduced the Iba1-labeled area in CFA animals, suggesting that TFAFA4 exerts its antinociceptive action by triggering a reduction in microglial activation.

Our finding that TFAFA4 acts through microglia is further reinforced by the recent identification of a putative receptor of TFAFA4, the FPR1 (Wang et al., 2015), which is located on cells deriving from myeloid lineage (Dorward et al., 2015; Gavins, 2010). Surprisingly, however, in most studies (Dorward et al., 2015; Hauser et al., 2010; Raouf et al., 2010; Wang et al., 2015), activation of FPR1 is believed to promote macrophage activation, macrophage phagocytosis, and the production of reactive oxygen species. In our experiments, we found that TFAFA4 rather promotes a decrease in the surface occupied by microglia in lamina II, suggesting a reduction in microglial activation. Several factors may account for this paradoxical effect. First, the effects of TFAFA4 on macrophage activation are known to be highly dependent upon its concentration (Wang et al., 2015). Second, discrepancies in the reaction of macrophages and microglia to a given stimulus may often be observed (Hooper et al., 2009; Durafourt et al., 2012).

### Displacing Inhibitory Synapses with Microglia?

Disruption of GABAergic transmission is a well-known phenomenon in pathological pain. However, the mechanisms involved in this disinhibition are still a matter of debate. In neuropathic pain models, a loss of GABAergic neurons (Todd, 2015; Taylor, 2009), a downregulation of the GABA synthesis enzyme (Moore et al., 2002), or a decrease in synaptic strength due to a shift in chloride reversal potential (Coull et al., 2005) have been proposed to contribute to this disinhibition. Although some of these mechanisms may exist in inflammatory pain models (Zhang et al., 2013), much less is known about GABAergic disinhibition in them. Several studies have reported a direct effect of inflammatory mediators on glycinergic transmission (Ahmadi et al., 2002; Kawasaki et al., 2008). This reduction in glycinergic inhibitory transmission may be accompanied by a shift in inhibitory transmission toward GABAergic transmission. Our immunocytochemical analysis highly suggests that, in addition to these mechanisms, CFA inflammation induces a decrease in the density of inhibitory synapses on lamina II somata that is reversed by

intrathecal injection of TFAFA4. Interestingly, no change in the excitatory synapse marker Homer was observed, highlighting the specificity of this mechanism to inhibitory inputs. Given that, in our experimental conditions, the density of inhibitory synapses mirrored the extension of microglial cells, it is tempting to speculate that the extension of microglial cells in CFA-inflamed animals induces a displacement of inhibitory synapses (synaptic stripping) and that TFAFA4 enables the restoration of these inhibitory synapses in lamina II by reducing microglial spreading, thus reinforcing inhibitory tonus and providing anti-nociception. Synaptic stripping was first identified in a facial nerve injury model by Blinzinger and Kreutzberg (1968) before the phenomenon was generalized to other structures and pathological models (Chen et al., 2014; Trapp et al., 2007). Although the release of pro-inflammatory substances may also be involved in the regulation of inhibitory transmission by microglia under the control of TFAFA4 (Ahmadi et al., 2002; Kawasaki et al., 2008), our data highlight a central mechanism in the regulation of pain transmission by microglial cells.

### EXPERIMENTAL PROCEDURES

Detailed procedures are available in the [Supplemental Experimental Procedures](#).

#### Animals

Protocols were approved by the local ethics committee (ref. 50120155A). C57BL/6J and TFAFA4<sup>Venus+/-</sup> mice were maintained under standard housing conditions (22°C, 40% humidity, 12-hr/12-hr light-dark cycle, and unlimited access to food and water). Experiments were performed on male animals except for *in vitro* electrophysiology, where both male and females were used.

#### In Vitro Electrophysiology

Patch-clamp recordings were performed at 31°C on 300- $\mu$ m spinal slices of young animals (postnatal day [P]17–P30) in warm aCSF (31°C) under infrared visual control, using KGlu-based (for EPSCs) or KCl-based (for IPSCs) internal solutions. Spontaneous and miniature synaptic events were analyzed using spike2 and visually filtered blind to experimental conditions.

#### In Vivo Electrophysiology

T13 and L1 vertebrae and dura mater were removed from deeply anesthetized mice (isoflurane, 2.5%), and superficial dorsal horn neurons were recorded with a glass electrode while stimulating the right hindpaw with Von Frey hairs. Drugs were injected through a second glass pipette inserted in the vicinity of the recording site.

#### Behavioral Assays

Mechanical allodynia and hyperalgesia were assessed on 8-week-old littermate males with Von Frey hairs using the “up and down method.” Intrathecal injection of recombinant TFAFA4, CGP, and phaclofen was performed in awake animals.

#### Electron Microscopy

Adult TFAFA4<sup>Venus+/-</sup> heterozygous mice were fixed with 4% paraformaldehyde and 0.5% glutaraldehyde. Sections were single, double, and/or triple stained following a conventional post-embedding protocol with antibodies raised against GABA, Venus, and VGluT3 and observed on a JEM-1010 transmission electron microscope.

#### Tissue Sections and Immunofluorescence

Immunofluorescence experiments were carried out using standard protocols. Images were acquired on an SPE Leica confocal microscope and analyzed with ImageJ. Sample preparation, acquisition, and analysis were performed blind to the experimental conditions.

## Statistics

Datasets were compared using either the Kolmogorov Smirnov test, Student's paired *t* test, or its non-parametric counterpart (Wilcoxon signed-rank test). When comparing more than two datasets, ANOVA (one-way, two-way, or repeated-measures) was used (see figure legends).  $p < 0.05$  was considered as statistically different.

## SUPPLEMENTAL INFORMATION

Supplemental Information includes Supplemental Experimental Procedures and five figures and can be found with this article online at <https://doi.org/10.1016/j.celrep.2018.02.068>.

## ACKNOWLEDGMENTS

This work was supported by ANR C-LTMR (ANR-14-CE13-0007), a doctoral fellowship from the French Ministry of Higher Education and Research, and a Labex BRAIN fellowship to C.K. Confocal microscopy studies were performed at the Bordeaux Imaging Center, a core facility of the national infrastructure France-BioImaging (ANR-10-INBS-04, France-BioImaging).

## AUTHOR CONTRIBUTIONS

C.K. and Y.L.F. designed the project; performed *in vitro* electrophysiology, behavioral assays, and immunofluorescence; and wrote the paper. O.R.-L. and C.K. performed *in vivo* electrophysiology. C.S. and A.M. performed electron microscopy. C.K., Y.L.F., M.L., O.R.-L., and C.S. analyzed data.

## DECLARATION OF INTERESTS

The authors declare no competing interests.

Received: September 18, 2017

Revised: January 19, 2018

Accepted: February 15, 2018

Published: March 13, 2018

## REFERENCES

- Ahmadi, S., Lippross, S., Neuhuber, W.L., and Zeilhofer, H.U. (2002). PGE(2) selectively blocks inhibitory glycinergic neurotransmission onto rat superficial dorsal horn neurons. *Nat. Neurosci.* *5*, 34–40.
- Baba, H., Ji, R.-R., Kohno, T., Moore, K.A., Ataka, T., Wakai, A., Okamoto, M., and Woolf, C.J. (2003). Removal of GABAergic inhibition facilitates polysynaptic A fiber-mediated excitatory transmission to the superficial spinal dorsal horn. *Mol. Cell. Neurosci.* *24*, 818–830.
- Bardoni, R., Ghirri, A., Salio, C., Prandini, M., and Merighi, A. (2007). BDNF-mediated modulation of GABA and glycine release in dorsal horn lamina II from postnatal rats. *Dev. Neurobiol.* *67*, 960–975.
- Blinzinger, K., and Kreutzberg, G. (1968). Displacement of synaptic terminals from regenerating motoneurons by microglial cells. *Z. Zellforsch. Mikrosk. Anat.* *85*, 145–157.
- Chen, Z., Jalabi, W., Hu, W., Park, H.-J., Gale, J.T., Kidd, G.J., Bernatowicz, R., Gossman, Z.C., Chen, J.T., Dutta, R., and Trapp, B.D. (2014). Microglial displacement of inhibitory synapses provides neuroprotection in the adult brain. *Nat. Commun.* *5*, 4486.
- Chéry, N., and De Koninck, Y. (1999). Junctional versus extrajunctional glycine and GABA(A) receptor-mediated IPSCs in identified lamina I neurons of the adult rat spinal cord. *J. Neurosci.* *19*, 7342–7355.
- Clark, A.K., Gruber-Schoffnegger, D., Drdla-Schutting, R., Gerhold, K.J., Malcangio, M., and Sandkühler, J. (2015). Selective activation of microglia facilitates synaptic strength. *J. Neurosci.* *35*, 4552–4570.
- Coull, J.A.M., Beggs, S., Boudreau, D., Boivin, D., Tsuda, M., Inoue, K., Gravel, C., Salter, M.W., and De Koninck, Y. (2005). BDNF from microglia causes the shift in neuronal anion gradient underlying neuropathic pain. *Nature* *438*, 1017–1021.
- Craig, A.D., and Bushnell, M.C. (1994). The thermal grill illusion: unmasking the burn of cold pain. *Science* *265*, 252–255.
- Daniele, C.A., and MacDermott, A.B. (2009). Low-threshold primary afferent drive onto GABAergic interneurons in the superficial dorsal horn of the mouse. *J. Neurosci.* *29*, 686–695.
- Delfini, M.-C., Mantilleri, A., Gaillard, S., Hao, J., Reynders, A., Malapert, P., Alonso, S., François, A., Barrere, C., Seal, R., et al. (2013). TAF4A, a chemokine-like protein, modulates injury-induced mechanical and chemical pain hypersensitivity in mice. *Cell Rep.* *5*, 378–388.
- Dorward, D.A., Lucas, C.D., Chapman, G.B., Haslett, C., Dhaliwal, K., and Rossi, A.G. (2015). The role of formylated peptides and formyl peptide receptor 1 in governing neutrophil function during acute inflammation. *Am. J. Pathol.* *185*, 1172–1184.
- Duan, B., Cheng, L., Bourane, S., Britz, O., Padilla, C., Garcia-Campany, L., Krashes, M., Knowlton, W., Velasquez, T., Ren, X., et al. (2014). Identification of spinal circuits transmitting and gating mechanical pain. *Cell* *159*, 1417–1432.
- Durafourt, B.A., Moore, C.S., Zammit, D.A., Johnson, T.A., Zaguia, F., Guiot, M.-C., Bar-Or, A., and Antel, J.P. (2012). Comparison of polarization properties of human adult microglia and blood-derived macrophages. *Glia* *60*, 717–727.
- Gavins, F.N.E. (2010). Are formyl peptide receptors novel targets for therapeutic intervention in ischaemia-reperfusion injury? *Trends Pharmacol. Sci.* *31*, 266–276.
- Guo, D., and Hu, J. (2014). Spinal presynaptic inhibition in pain control. *Neuroscience* *283*, 95–106.
- Harvey, K., Duguid, I.C., Alldred, M.J., Beatty, S.E., Ward, H., Keep, N.H., Lingenfelter, S.E., Pearce, B.R., Lundgren, J., Owen, M.J., et al. (2004). The GDP-GTP exchange factor collybistin: an essential determinant of neuronal gephyrin clustering. *J. Neurosci.* *24*, 5816–5826.
- Hauser, C.J., Sursal, T., Rodriguez, E.K., Appleton, P.T., Zhang, Q., and Itagaki, K. (2010). Mitochondrial damage associated molecular patterns from femoral reamings activate neutrophils through formyl peptide receptors and P44/42 MAP kinase. *J. Orthop. Trauma* *24*, 534–538.
- Hooper, C., Pinteaux-Jones, F., Fry, V.A.H., Sevastou, I.G., Baker, D., Heales, S.J., and Pocock, J.M. (2009). Differential effects of albumin on microglia and macrophages; implications for neurodegeneration following blood-brain barrier damage. *J. Neurochem.* *109*, 694–705.
- Hui, J., Zhang, Z.-J., Zhang, X., Shen, Y., and Gao, Y.-J. (2013). Repetitive hyperbaric oxygen treatment attenuates complete Freund's adjuvant-induced pain and reduces glia-mediated neuroinflammation in the spinal cord. *J. Pain* *14*, 747–758.
- Ji, R.-R., Berta, T., and Nedergaard, M. (2013). Glia and pain: is chronic pain a gliopathy? *Pain* *154* (Suppl 1), S10–S28.
- Kawasaki, Y., Zhang, L., Cheng, J.-K., and Ji, R.-R. (2008). Cytokine mechanisms of central sensitization: distinct and overlapping role of interleukin-1 $\beta$ , interleukin-6, and tumor necrosis factor- $\alpha$  in regulating synaptic and neuronal activity in the superficial spinal cord. *J. Neurosci.* *28*, 5189–5194.
- Keller, A.F., Coull, J.A., Chery, N., Poisbeau, P., and De Koninck, Y. (2001). Region-specific developmental specialization of GABA-glycine cosynapses in laminae I-II of the rat spinal dorsal horn. *J. Neurosci.* *21*, 7871–7880.
- Laffray, S., Bouali-Benazzouz, R., Papon, M.-A., Favereaux, A., Jiang, Y., Holm, T., Spriet, C., Desbarats, P., Fossat, P., Le Feuvre, Y., et al. (2012). Impairment of GABAB receptor dimer by endogenous 14-3-3 $\zeta$  in chronic pain conditions. *EMBO J.* *31*, 3239–3251.
- Latreoliere, A., and Woolf, C.J. (2009). Central sensitization: a generator of pain hypersensitivity by central neural plasticity. *J. Pain* *10*, 895–926.
- Leitner, J., Westerholz, S., Heinke, B., Forsthuber, L., Wunderbaldinger, G., Jäger, T., Gruber-Schoffnegger, D., Braun, K., and Sandkühler, J. (2013). Impaired excitatory drive to spinal GABAergic neurons of neuropathic mice. *PLoS ONE* *8*, e73370.

- Li, L., Rutlin, M., Abaira, V.E., Cassidy, C., Kus, L., Gong, S., Jankowski, M.P., Luo, W., Heintz, N., Koerber, H.R., et al. (2011). The functional organization of cutaneous low-threshold mechanosensory neurons. *Cell* 147, 1615–1627.
- Liao, H.-Y., Hsieh, C.-L., Huang, C.-P., and Lin, Y.-W. (2017). Electroacupuncture attenuates CFA-induced inflammatory pain by suppressing Nav1.8 through S100B, TRPV1, opioid, and adenosine pathways in mice. *Sci. Rep.* 7, 42531.
- Lin, Q., Peng, Y.B., and Willis, W.D. (1996). Possible role of protein kinase C in the sensitization of primate spinothalamic tract neurons. *J. Neurosci.* 16, 3026–3034.
- Lin, T., Li, K., Zhang, F.-Y., Zhang, Z.-K., Light, A.R., and Fu, K.-Y. (2007). Dissociation of spinal microglia morphological activation and peripheral inflammation in inflammatory pain models. *J. Neuroimmunol.* 192, 40–48.
- Lu, Y., and Perl, E.R. (2005). Modular organization of excitatory circuits between neurons of the spinal superficial dorsal horn (laminae I and II). *J. Neurosci.* 25, 3900–3907.
- Lu, Y., Dong, H., Gao, Y., Gong, Y., Ren, Y., Gu, N., Zhou, S., Xia, N., Sun, Y.-Y., Ji, R.-R., and Xiong, L. (2013). A feed-forward spinal cord glycinergic neural circuit gates mechanical allodynia. *J. Clin. Invest.* 123, 4050–4062.
- Lumpkin, E.A., Marshall, K.L., and Nelson, A.M. (2010). The cell biology of touch. *J. Cell Biol.* 191, 237–248.
- Mackenzie, R.A., Burke, D., Skuse, N.F., and Lethlean, A.K. (1975). Fibre function and perception during cutaneous nerve block. *J. Neurol. Neurosurg. Psychiatry* 38, 865–873.
- Melzack, R., and Wall, P.D. (1965). Pain mechanisms: a new theory. *Science* 150, 971–979.
- Mirauccourt, L.S., Dallel, R., and Voisin, D.L. (2007). Glycine inhibitory dysfunction turns touch into pain through PKCgamma interneurons. *PLoS ONE* 2, e1116.
- Moore, K.A., Kohno, T., Karchewski, L.A., Scholz, J., Baba, H., and Woolf, C.J. (2002). Partial peripheral nerve injury promotes a selective loss of GABAergic inhibition in the superficial dorsal horn of the spinal cord. *J. Neurosci.* 22, 6724–6731.
- O'Brien, J.A., and Berger, A.J. (1999). Cotransmission of GABA and glycine to brain stem motoneurons. *J. Neurophysiol.* 82, 1638–1641.
- Polgár, E., Durrieux, C., Hughes, D.I., and Todd, A.J. (2013). A quantitative study of inhibitory interneurons in laminae I–III of the mouse spinal dorsal horn. *PLoS ONE* 8, e78309.
- Qi, J., Chen, C., Meng, Q.-X., Wu, Y., Wu, H., and Zhao, T.-B. (2016). Crosstalk between activated microglia and neurons in the spinal dorsal horn contributes to stress-induced hyperalgesia. *Sci. Rep.* 6, 39442.
- Raghavendra, V., Tanga, F.Y., and DeLeo, J.A. (2004). Complete Freund's adjuvant-induced peripheral inflammation evokes glial activation and proinflammatory cytokine expression in the CNS. *Eur. J. Neurosci.* 20, 467–473.
- Raoof, M., Zhang, Q., Itagaki, K., and Hauser, C.J. (2010). Mitochondrial peptides are potent immune activators that activate human neutrophils via FPR-1. *J. Trauma* 68, 1328–1334.
- Ribeiro-da-Silva, A. (2004). Substantia gelatinosa of the spinal cord. In *The Rat Nervous System*, 3rd, G. Paxinos, ed. (Academic Press), pp. 129–148.
- Sdrulla, A.D., Xu, Q., He, S.-Q., Tiwari, V., Yang, F., Zhang, C., Shu, B., Shechter, R., Raja, S.N., Wang, Y., et al. (2015). Electrical stimulation of low-threshold afferent fibers induces a prolonged synaptic depression in lamina II dorsal horn neurons to high-threshold afferent inputs in mice. *Pain* 156, 1008–1017.
- Seal, R.P., Wang, X., Guan, Y., Raja, S.N., Woodbury, C.J., Basbaum, A.I., and Edwards, R.H. (2009). Injury-induced mechanical hypersensitivity requires C-low threshold mechanoreceptors. *Nature* 462, 651–655.
- Spike, R.C., and Todd, A.J. (1992). Ultrastructural and immunocytochemical study of lamina II islet cells in rat spinal dorsal horn. *J. Comp. Neurol.* 323, 359–369.
- Sun, S., Cao, H., Han, M., Li, T.-T., Pan, H.-L., Zhao, Z.-Q., and Zhang, Y.-Q. (2007). New evidence for the involvement of spinal fractalkine receptor in pain facilitation and spinal glial activation in rat model of monoarthritis. *Pain* 129, 64–75.
- Takazawa, T., and MacDermott, A.B. (2010). Glycinergic and GABAergic tonic inhibition fine tune inhibitory control in regionally distinct subpopulations of dorsal horn neurons. *J. Physiol.* 588, 2571–2587.
- Takazawa, T., Choudhury, P., Tong, C.-K., Conway, C.M., Scherrer, G., Flood, P.D., Mukai, J., and MacDermott, A.B. (2017). Inhibition mediated by glycinergic and GABAergic receptors on excitatory neurons in mouse superficial dorsal horn is location-specific but modified by inflammation. *J. Neurosci.* 37, 2336–2348.
- Taylor, B.K. (2009). Spinal inhibitory neurotransmission in neuropathic pain. *Curr. Pain Headache Rep.* 13, 208–214.
- Todd, A.J. (2015). Plasticity of inhibition in the spinal cord. *Handb. Exp. Pharmacol.* 227, 171–190.
- Todd, A.J., Watt, C., Spike, R.C., and Sieghart, W. (1996). Colocalization of GABA, glycine, and their receptors at synapses in the rat spinal cord. *J. Neurosci.* 16, 974–982.
- Trapp, B.D., Wujek, J.R., Criste, G.A., Jalabi, W., Yin, X., Kidd, G.J., Stohlman, S., and Ransohoff, R. (2007). Evidence for synaptic stripping by cortical microglia. *Glia* 55, 360–368.
- Wang, W., Li, T., Wang, X., Yuan, W., Cheng, Y., Zhang, H., Xu, E., Zhang, Y., Shi, S., Ma, D., and Han, W. (2015). FAM19A4 is a novel cytokine ligand of formyl peptide receptor 1 (FPR1) and is able to promote the migration and phagocytosis of macrophages. *Cell. Mol. Immunol.* 12, 615–624.
- Woolf, C.J. (2011). Central sensitization: implications for the diagnosis and treatment of pain. *Pain* 152 (3, Suppl), S2–S15.
- Xu, F., Li, Y., Li, S., Ma, Y., Zhao, N., Liu, Y., Qian, N., Zhao, H., and Li, Y. (2014). Complete Freund's adjuvant-induced acute inflammatory pain could be attenuated by triptolide via inhibiting spinal glia activation in rats. *J. Surg. Res.* 188, 174–182.
- Yarnitsky, D., and Ochoa, J.L. (1990). Release of cold-induced burning pain by block of cold-specific afferent input. *Brain* 113, 893–902.
- Zhang, Z., Wang, X., Wang, W., Lu, Y.-G., and Pan, Z.Z. (2013). Brain-Derived Neurotrophic Factor-Mediated Downregulation of Brainstem K<sup>+</sup>-Cl<sup>-</sup> Cotransporter and Cell-Type-Specific GABA Impairment for Activation of Descending Pain Facilitation. *Mol. Pharmacol.* 84, 511–520.